To Fold or Not to Fold?

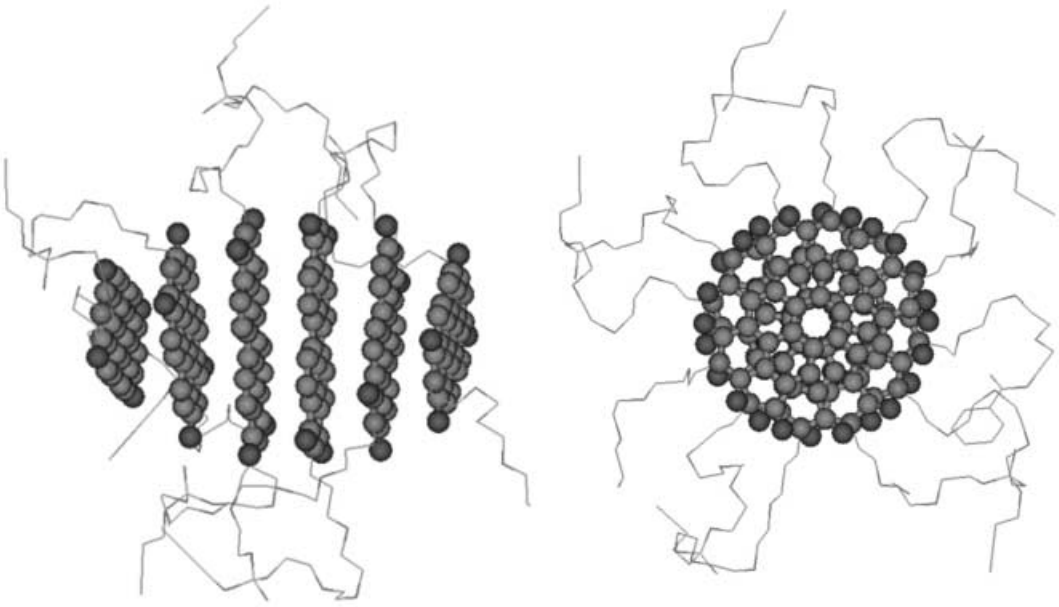

Folded nanostructures

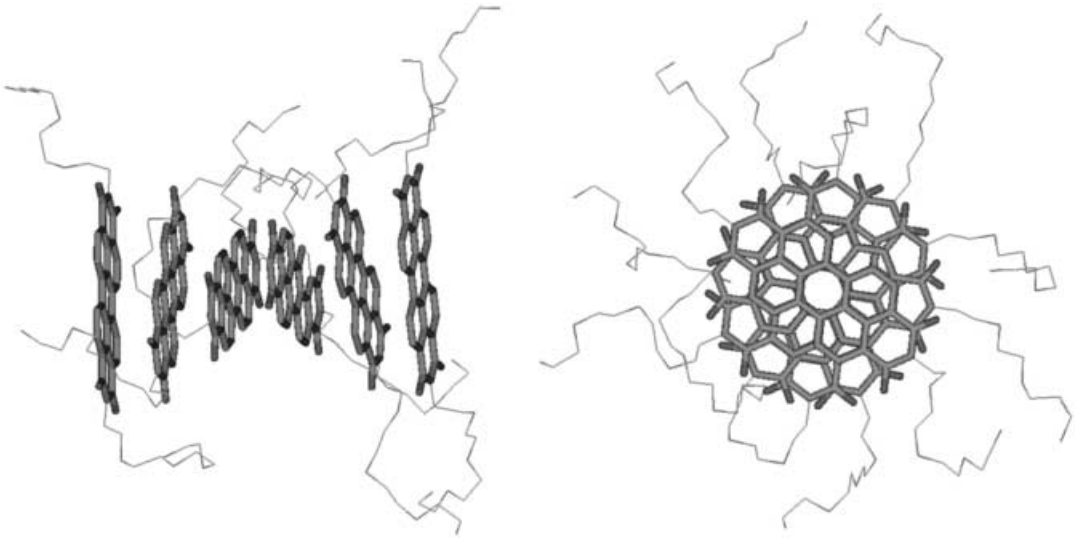

Self-assembled nanostructures

Nature uses folded *biopolymers* and their assemblies to
- catalyze reactions and amplify chemical information
- repair DNA damage and transmit information

Can *synthetic polymers* meet the same challenge?

© 2003 Wiley-VCH Verlag GmbH & Co. KGaA, Weinheim
DOI: 10.1002/chem.200305025 *Chem. Eur. J.* **2003**, *9*, 4594 – 4601

Folding versus Self-Assembling

Alexander D. Q. Li,*[a] Wei Wang,[a] and Li-Qiong Wang[b]

Abstract: Model foldable polymers with sequences of rigid hydrophobic chromophores and flexible hydrophilic tetra(ethylene glycol) were synthesized and used as a paradigm for studying molecular-folding and self-assembly phenomena. Our results demonstrate that intramolecular association or folding prevails over intermolecular interaction or self-assembling in the concentration region from 1 μM to 0.1M. Importantly, folded polymeric nanostructures have absorption and fluorescence properties that are distinct from those of unfolded polymers or free monomers. We hypothesize that the origins of folding and self-assembly come from interactions between molecular units, and that the key parameter that regulates the on-and-off of such interactions is the distance R separating the two molecular units. Each molecular unit produces a characteristic force field, and when another molecular unit enters this field, the probability that the two units will interact increases significantly. A preliminary estimate of the radius of such a force field for the perylene tetracarboxylic diimide chromophore is about 90–120 Å. As a result, phenomena associated with folding or self-assembly of molecular species are observed when these conditions are met in solution.

Keywords: foldable polymer · protein engineering · protein folding · self-assembly · synthesis design

Introduction

Nature utilizes folding and self-assembly (SA) strategies extensively in biological systems. Indeed, correctly folded biopolymers have generated an astonishing array of novel functions, including protein catalytic reactions,[1] cell regulation, DNA repair,[2] information storage,[3] and self-replication. While biopolymers can accomplish natural wonders, can synthetic polymers meet the same challenges? In principle, synthetic polymers can be designed to form folded nanostructures with useful functions as well.[4–8] Whereas, great scientific advances in synthetic macromolecules have been achieved by using conjugated polymers with interesting photoluminescence properties,[9–16] our current knowledge about folding synthetic polymers is at a very primitive stage and has only recently begun to be understood.[17] Biopolymers are adept at information coding, specific folding, and recognition; synthetic polymers offer the promise of incorporating additional interesting properties, such as those involving light-emitting capabilities. The folding and unfolding of synthetic polymers can be conveniently monitored by using their interesting optical properties, whereas biopolymers are seldom colored and frequently need to be tagged with fluorescence chromophores for studying conformation changes. Understanding polymer folding "codes" could guide us in protein engineering and the design of novel foldable polymers with functions that biopolymers do not even have. In this paper, we report the competition between intramolecular attraction (folding) and intermolecular attraction (self-assembling) in alternating hydrophobic and hydrophilic sequences. We have chosen the planar perylene tetracarboxylic diimide (PTD) unit as the rigid hydrophobic chromophore and tetra(ethylene glycol) as the foldable hinge.

[a] Prof. A. D. Q. Li, Dr. W. Wang
Department of Chemistry and Center for Materials Research
Washington State University, Pullman, WA 99164 (USA)
Fax: (+1) 509-335-8867
E-mail: dequan@wsu.edu

[b] Dr. L.-Q. Wang
Material Science Division, Pacific Northwest National Laboratory
Richland, WA 99352 (USA)

The Design of Foldable Polymers

Our strategy to prepare foldable polymers is to alternate a flexible region and a rigid hydrophobic chromophore region. Both regions should have a well-defined sequence and length, preferably in the nanometer range, so that the folded polymers form "smart" nanostructured materials. The requirements for the foldable regions are that they possess flexibility, hydrophilicity, and solubility in water or organic solvents. Suitable sequences for the foldable regions are oligo(ethylene glycol) (OEG) and oligo deoxyribonucleic acid (DNA). OEGs are soluble in both organic and aqueous solutions and hence suitable for folding studies in both organic and aqueous phases, whereas DNA is only soluble in aqueous solutions so foldable polymers with extensive DNA sequences can only be investigated in water. On the other hand, the requirement for the hydrophobic regions is the

 DOI: 10.1002/chem.200305025 © 2003 Wiley-VCH Verlag GmbH & Co. KGaA, Weinheim

ability to pack into ordered structures. The chromophore sequences should also have interesting optical properties, absorption and/or fluorescence, which serve to report structural changes.

One of the central ideas of our design is to use attractive forces between chromophores to create folded nanostructures. These forces could be molecular orbital overlaps such as $\pi-\pi$ interactions or could come from hydrophobic effects. In the initial experiments, we used flexible OEG to minimize appreciable molecular interactions in the foldable regions and focus on the interactions of the chromophores. Under this circumstance, the chromophores can either interact intramolecularly or intermolecularly. If the chromophores interact intramolecularly, the polymer will fold first (Scheme 1). However, if the chromophores interact intermolecularly, the polymer will self-assemble first. The central question is will

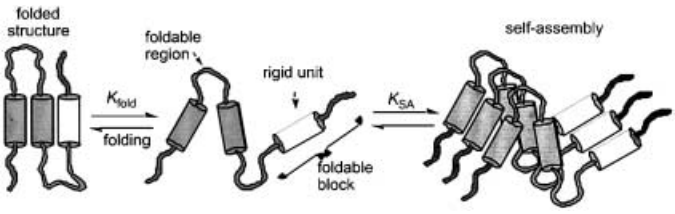

Scheme 1. Attractions between the chromophoric blocks could result in either folded or self-assembled nanostructures. Intramolecular attractions favor folding while intermolecular interactions favor self-assembly.

the polymer fold or will it self-assemble? The consequence of this outcome could be significant. If folding prevails, one can design individual foldable molecular machinery for probing mechanisms of interest or use folded polymers as nanoscale building blocks for advanced materials. However, if self-assembly prevails,[18] the foldable polymer will form highly ordered molecular assemblies that cause loss of the individual character of the folded polymer.

Here, we present simple thermodynamic arguments about folding versus self-assembly. Since folding is a unimolecular process and self-assembly is a multimolecular process, one cannot directly compare the equilibrium constants of K_{fold} and K_{SA} to determine which process is dominant. For example, assuming that the concentrations of *all* folded, unfolded, and self-assembled structures were 1 mM, we would have $K_{fold}=1$ and $K_{SA}(\text{dimer})=1000\,\text{M}^{-1}$ or $K_{SA}(\text{trimer})=1\,000\,000\,\text{M}^{-2}$, etc. Apparently, larger self-assembly equilibrium constants do not reflect larger concentrations of self-assembled products. Experimentally, we have measured $K_{fold}=6.2$ and $K_{SA}=31\text{M}^{-1}$ for the perylene-based foldable polymer in 1,1,2,2-tetrachloroethane. To understand which process is favored thermodynamically, we examine the simplest case: the folding or self-assembling of dimers. To a first-order approximation, we can assume that the interaction forces of both folding and self-assembly are of the same origin.[19, 20] In other words, the enthalpy due to chromophore units of the folding process is approximately the same as the enthalpy of the self-assembling process, $\Delta H_o^{fold}\approx\Delta H_o^{SA}$. However, the entropy of folding and self-assembly are quite different because, in the case of folding, the two chromophores are covalently bound together and in close proximity, whereas the two chromophores could be far apart in the case of self-assembly. Consider a folding process of A-A $\leftrightarrow$ A_2, in which A is the monomeric unit, the change of entropy is expressed as $\Delta S_o^{fold}=S(A_2)-S(\text{A-A})$. Similarly consider a SA process of A + A $\leftrightarrow$ A:A, in which A is the monomer (e.g., **1b**), the change of entropy is described as $\Delta S_o^{SA}=S(\text{A:A})-2S(\text{A})$. It is reasonable to assume that the folded dimer resembles the self-assembled dimer, thus their entropies are approximately equal, $S(A_2)\approx S(\text{A:A})$. Based on these approximations, we conclude that $\Delta S_o^{fold}-\Delta S_o^{SA}=2S(\text{A})-S(\text{A-A})>0$, thus, $\Delta S_o^{fold}>\Delta S_o^{SA}$. To summarize, folding is favored by entropy and thermodynamic analysis argues that folding precedes self-assembly.

Foldable Polymer Synthesis

Folding requires that the polymer should possess multiple units within the backbone with mutual attractions. In addition, these units should be linked with flexible molecular spacers that function as hinges. Due to these requirements, radical and anionic polymerizations are currently not suitable for constructing foldable polymers with large chromophores in the backbone. Therefore, we have identified three strategies for developing foldable polymers containing optically active chromophores in the main chain. The first approach is solution synthesis of alternating sequences of rigid hydrophobic chromophores and flexible hydrophilic spacers. This approach employs the traditional condensation polymerization technique. The polymer resulting from this method has alternating sequences originating from the two monomers, and its molecular weight typically has a wide distribution. The advantage of this method is that the polymerization is convenient, and the drawback is that the lengths of the final polymers are ill-defined. Individual folding actions and quantum interactions are overwhelmed by the ensemble effect.

The second approach is a stepwise solid-state method.[21] This method employs two key components: a solid support such as beads or porous glass and one or more asymmetric building blocks with one end activated and the other end protected. The foldable polymer can be grown on a solid support by adding one asymmetric building block at a time. Typically, the growing end is protected so that only one desired building block is added each time. To grow the polymer chain, the protected group is removed after each coupling and the terminal of the polymer chain is available for extension again. After the desired number of building blocks has been incorporated, the foldable polymer can be cleaved from the support to yield a monodispersed polymer. The advantage of this method is that the lengths of all the macromolecules are identical. The disadvantage is that the quantity of the final polymer is small, even when the yield of each coupling step is very high. Nonetheless, oligonucleotides and peptides are routinely synthesized by using this method.

The third approach is a stepwise solution-phase synthesis.[22] Again, this method requires an asymmetric building block with one end activated and the other end protected. Instead of coupling to a solid support, we attached the building block

© 2003 Wiley-VCH Verlag GmbH & Co. KGaA, Weinheim

to a molecule that serves as a polymer chain anchor. Here we have developed a stepwise solution approach for constructing foldable polymers in which the molecular weight can be controlled as in the solid-phase synthesis. The unique properties of such polymers are their single molecular weight and precisely controlled sequences, orientations, and folding.

Although the above three strategies provide general guidance, the tactics to implement them in the construction of alternative rigid and flexible sequences still remain critical. One approach is to alternatively couple the rigid sequence to the flexible sequence in order to construct foldable polymers. However, the problem may arise that the rigid sequence becomes so insoluble as to render the coupling reaction low-yielding and ill-defined. Another approach is to sandwich the rigid sequence between two half flexible sequences and initiate the coupling between the two flexible ends. The opposite of this tactic is to sandwich the flexible sequence with two half rigid sequences and carry out coupling reactions between the two rigid ends. There are known reactions, such as Wittig or Suzuki coupling, that will yield conjugated rigid sequences, but we decided to employ oligo(ethylene glycol) as the flexible chains and use phosphoramidite chemistry to connect them. The main reasons are that phosphoramidite chemistry produces high yields and the coupling of soft chains is relatively easier than that of rigid chromophores, especially for macromolecules.

Accordingly, we attached flexible tetra(ethylene glycol) to a large rigid perylene tetracarboxylic dianhydride to form the flexible-rigid-flexible structure. We first activated one hydroxyl of the tetra(ethylene glycol) by the action of tosylation, which yields the monotosylation product of tetra(ethylene glycol). The tosylate was subsequently replaced with an azido group. Reduction of the azide yielded 2-(2-(2-(2-amino ethoxy)ethoxy)ethoxy) ethanol,[23] which was condensed with perylene tetracarboxylic dianhydride to yield the desired flexible-rigid-flexible structure, bis-*N*,*N*′-(2-(2-(2-(2-hydroxyethoxy)ethoxy)ethoxy)ethyl) perylene tetracarboxylic diimide (**1a**).[24, 25] Applying the third strategy, we need to provide a chain anchor and an asymmetric building block. To form the polymer chain anchor, we further monobenzoylated bis-*N*,*N*′-(2-(2-(2-(2-hydroxyethoxy)ethoxy)ethoxy)ethyl) perylene tetracarboxylic diimide to produce **1b** so that polymeric chain extension is only permitted at the other hydroxy group (Scheme 2). To prepare the asymmetric building block, we protected only one hydroxyl group of bis-*N*,*N*′-(2-(2-(2-(2-hydroxyethoxy)ethoxy)ethoxy)ethyl) perylene tetracarboxylic diimide with 4,4′-dimethoxyl trityl (DMTr) to yield **1c**[26, 27] and activated the other hydroxyl group with phosphoramidite to yield **1d**.

The construction of foldable polymers was carried out by using the building block (**1d**) to attack the monobenzoylated anchor (**1c**) to synthesize a dimer with DMTr-protected chain end (**2a**). The DMTr group was subsequently removed by acid hydrolysis to generate the hydroxy group necessary for chain extension (**2b**).[28, 29] By using this method of coupling followed by detritylation, we prepared specific oligomers including dimers (**2a,b**), trimers (**3a,b**), tetramers (**4a,b**), pentamers (**5a,b**), and hexamers (**6a,b**). This is such an effective strategy that we have used it to further synthesize higher-order oligomers including heptamers (**7a**,**b**), octamers (**8a**,**b**), nonamers (**9a**,**b**), and even undecamers (**10a,b**).

Optical Absorption of Folded Polymers

One advantage of studying foldable polymers containing optically active chromophores is that they can be easily investigated with optical spectroscopy, and the resulting foldable polymer can be a functional sensor or biosensor. Folding of perylene units provides a new paradigm in this respect and is signaled by a diagnostic optical absorption change because both covalently bound perylene cyclophanes[30] and folded PTD oligomers[22] have an *inverse* intensity distributions among their vibronic states, $A^{0\rightarrow0}/A^{0\rightarrow1} = 0.7$, whereas free perylene molecules have *normal* Franck–Condon progressions with $A^{0\rightarrow0}/A^{0\rightarrow1} \approx 1.6$.[31, 32] Hence, the absorption ratio of the $0\rightarrow0$ to the $0\rightarrow1$ transition can be used to quantify the degree of folding in the perylene-containing polymers. Such remarkable intensity reversal was attributed to the strong electron–phonon coupling in the folded nanostructures as the absorption maximum blue shifts by 0.17 eV from the $0\rightarrow0$ transition to the $0\rightarrow1$ transition. The relative intensities of the vibronic bands are governed by the Franck–Condon factors. The intensity reversal indicates that the optimum overlap has shifted from $\langle\chi'_{v'=0}\,|\,\chi_{v=0}\rangle$ in free monomers to $\langle\chi'_{v'=1}\,|\,\chi_{v=0}\rangle$ in the folded structures. Here χ and χ' are the ground- and excited-state vibronic wave functions. The strong electron–phonon coupling indicates that the PTD molecules adopt largely eclipsed structures with interplanar distances less than van der Waals contact to establish quantum interactions of π-orbital overlaps.

As shown in Figure 1A, a dramatic change in optical absorption comes from the transition from monomer to dimer; the monomer has a ratio of $A^{0\rightarrow0}/A^{0\rightarrow1} \approx 1.6$ whereas the dimer has a ratio of $A^{0\rightarrow0}/A^{0\rightarrow1} = 0.92$ in chloroform. The reason is that the dimer can fold and exist as a folded structure at low concentrations. In contrast, the monomer cannot self-assemble at low concentrations (vide infra). A large decrease in the intensity ratio between the $0\rightarrow0$ and $0\rightarrow1$ transitions is also observed from dimer to trimer $A^{0\rightarrow0}/A^{0\rightarrow1} = 0.82$. The results in Figure 1A confirm that the optical absorption properties of a free PTD molecule are very different from a stack of two PTD molecules. Moreover, a three-layer PTD molecular sandwich produces an appreciable reduction in the $A^{0\rightarrow0}/A^{0\rightarrow1}$ value although its effects are not as pronounced as the initial bimolecular stacks. Additional PTD molecules added to the stacks continue to reduce the $A^{0\rightarrow0}/A^{0\rightarrow1}$ value, but to a much smaller extent. For instance the $A^{0\rightarrow0}/A^{0\rightarrow1}$ value for chromophoric hexamer is only about 0.72 in chloroform. The $A^{0\rightarrow0}/A^{0\rightarrow1}$ values for the monomer, dimer, trimer, tetramer, pentamer, and hexamer are 1.64, 0.92, 0.82, 0.78, 0.76, 0.72, respectively; the trend seems to indicate that it is slowly approaching to a limiting value.

Conversely, self-assembling of PTD monomers (**1**) does not happen at low concentrations. In Figure 1B, we show that optical absorption spectra are essentially the same when the monomer concentration is below 1 mM; this indicates that

 © 2003 Wiley-VCH Verlag GmbH & Co. KGaA, Weinheim

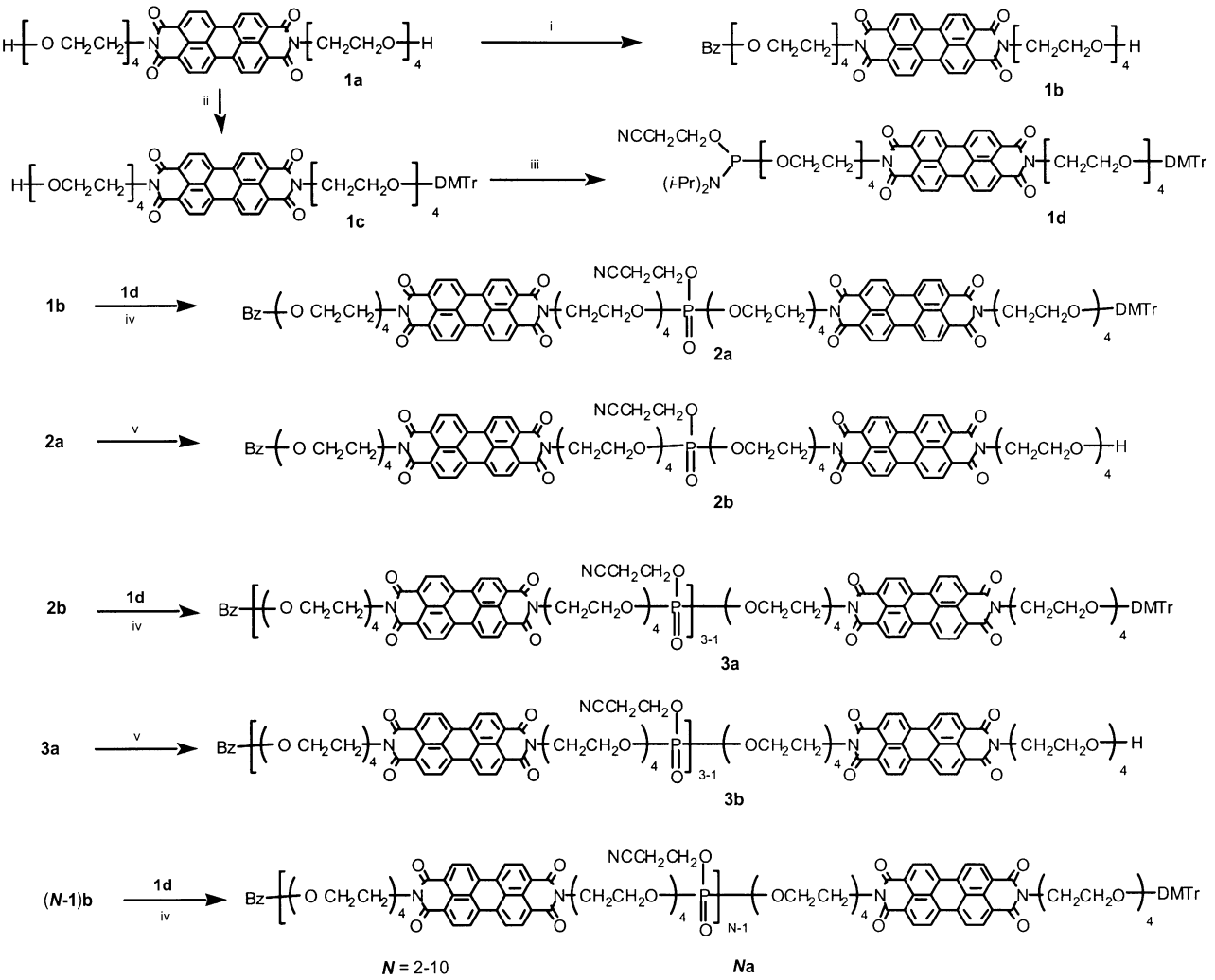

Scheme 2. Stepwise solution synthesis of foldable polymers. We carried out repeated attacks with the building block **1d** on a chain anchor (**1b**). Each attack added one chromophore unit to the growing end of the foldable polymer. i) benzoyl chloride/py; ii) 4,4′-dimethoxytrityl chloride/py; iii) 2-cyanoethyl diisopropylcholophosphoramidite/*N*,*N*-diisopropylethyl amine/CH_2Cl_2; iv) CH_2Cl_2/*N*-phenylimidazolium triflate, RT, then I_2 (CH_2Cl_2/py/H_2O 1:3:1), RT; v) $CHCl_2CO_2H/CH_2Cl_2$, RT.

there is no appreciable amount of self-organization under these conditions. However, the $0 \rightarrow 1$ transition begins to grow when the chromophore concentration is increased beyond a critical value of $C_C \approx 1$ mM; this indicates the onset of intermolecular association. At the critical concentration, there are ~ 2 molecules in a cube of $15 \times 15 \times 15$ nm^3. In such a box, the shortest distance between the two molecules is zero, the longest distance is ~ 25 nm, and the median is about 12.5 nm. The experimental results suggest that at such proximity, one molecule "feels" the presence of the other either through attractive forces (ΔH effect) or random collisions (ΔS effect). The introduction of a characteristic force field for each individual molecule provides a general rationale for self-organization and folding. If we use a spherical model instead of the cubic one, we find that, on average, two molecules are within a sphere with a radius of 9 nm at the onset of molecular self-organization. Therefore the force field for PTD molecules probably has an average radius in the range of 9–12 nm, and molecular self-organization occurs when the concentration drives intermolecular distance below this critical region. In the foldable polymers, the distance between two chromophore units is about 3–4 nm, and this value is far below the median value of 12.5 nm required for self-organization. This comparison leads to the conclusion that folding is favored because of close proximity of interacting groups. In other words, folding requires less reduction in entropy than the process of self-assembly; therefore folding is favored in solution according to the second law of thermodynamics.

NMR Studies of Folding and Self-Assembly Phenomena

Another advantage of studying self-assembled π-stacked aromatic chromophores is that the ring current in one chromophore induces a distinct chemical shift in the proton resonances of its stacked neighbors. As shown in Figure 2A, at low concentration (2.3 mM), compound **1b** exists as mostly "free" monomer as indicated by the sharp AA′BB′ patterns of the Ha and Hb protons; here Ha represents the four outer protons and Hb represents the four inner protons on the

© 2003 Wiley-VCH Verlag GmbH & Co. KGaA, Weinheim

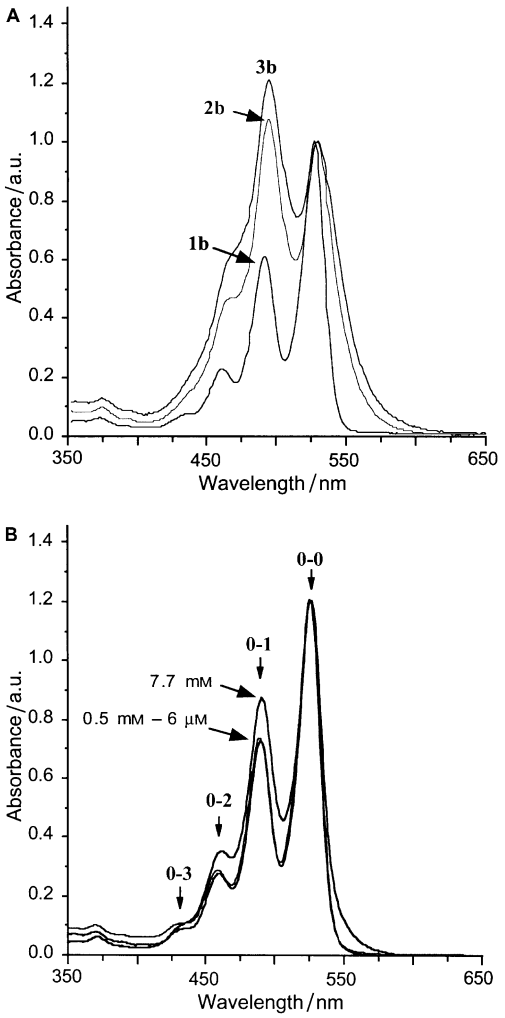

Figure 1. A) Normalized optical-absorption spectra of folded chromophoric dimer **2b** and trimer **3b** that have an intensity reversal between the $0 \rightarrow 0$ and $0 \rightarrow 1$ transitions when compared with the free monomer **1b**. The chromophoric unit concentrations are 6.6 μM for all oligomers. B) Normalized optical-absorption spectra of chromophoric monomer **1b** and its self-assembled products. At concentrations less than ~1 mM (0.5 mM and 6 μM shown), few self-assembled products are formed, as indicated by the absence of perturbation of the optical spectra. At concentrations above ~1 mM (7.7 mM shown), the $0 \rightarrow 1$ transition intensity begins to increase, indicating self-organization in solution.

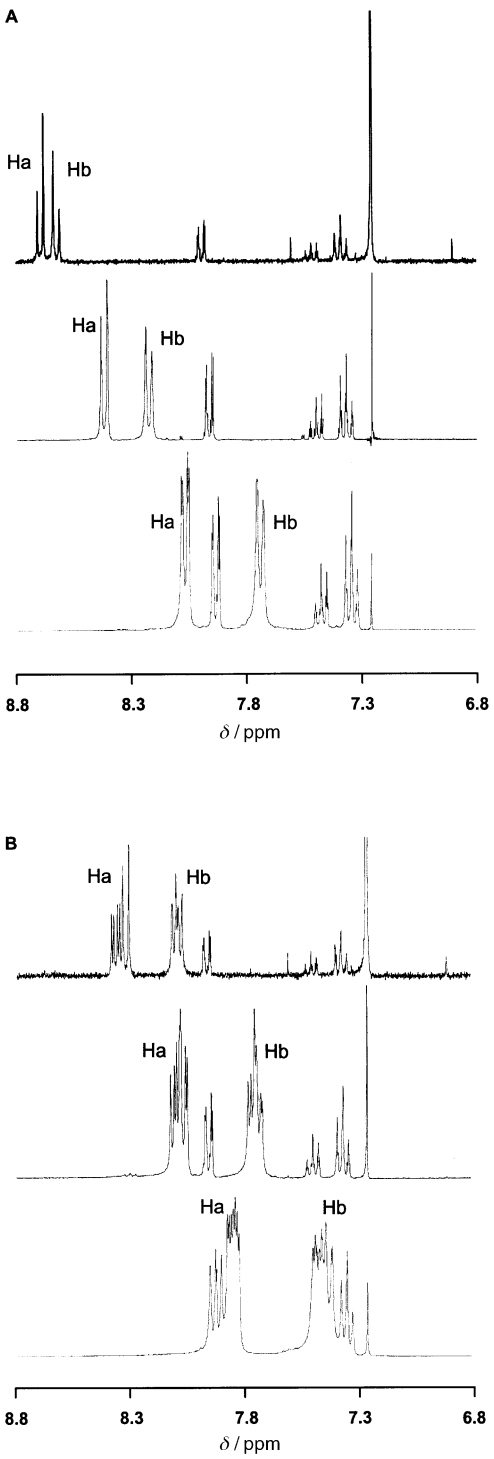

Figure 2. NMR spectra of A) monomer and B) folded dimer in the aromatic region. The concentrations of the monomer (**1b**) are 2.3 (top), 18 (middle), and 142 mM (bottom) while the concentrations of the dimer (**2b**) are 2.3 (top), 23 (middle), 94 mM (bottom). Note that the chemical-shift separation between Ha and Hb of the folded dimer (B) is much larger than that of free monomer (A) around the critical concentration (C_C) of self-assembly.

perylene ring. As the concentration increases beyond the critical value, three characteristic patterns associated with π-stacking emerged. First, we observed upfield shifts of both Ha and Hb. Second, we observed that the chemical-shift separation ($\Delta\delta = \delta(\mathrm{Ha}) - \delta(\mathrm{Hb})$) between Ha and Hb increases with concentration. Third, the peaks of Ha and Hb begin to broaden with additional fine structures; this indicates the presence of self-assembled dimers and higher oligomers. The NMR results demonstrate that free monomer, self-assembled dimer, trimer, etc. undergo rapid exchange on the NMR timescale. The fact that the NMR peaks are well resolved confirms that the system is in a dynamic equilibrium consisting of free monomer and various self-assembled oligomers. The critical concentration for the formation of self-assembled nanostructures is ~1 mM, which is in good agreement with the optical-absorption results.

Folded aromatic chromophores have essentially the same NMR characteristics as those self-assembled π-stacks. Therefore, we should expect that the Ha and Hb nuclear magnetic resonances shift upfield with increased separation ($\Delta\delta$) between Ha and Hb. Moreover, we expect fine splitting in

 © 2003 Wiley-VCH Verlag GmbH & Co. KGaA, Weinheim

Ha and Hb since the two chromophoric units are not equivalent. Indeed, the details of these phenomena are shown in Figure 2B. The larger $\Delta\delta$ values observed for the folded structures arise because the inner proton (Hb) experiences a larger ring-current than the outer proton (Ha) when the two aromatic rings are π-stacked. This makes the $\Delta\delta$ value a reliable indicator of folded versus nonfolded structures. For free monomer **1**, $\Delta\delta$ is 0.061 ppm, whereas, the $\Delta\delta$ values (Figure 3) for folded dimer, trimer, and tetramer are 0.26, 0.33, and 0.38 ppm, respectively.

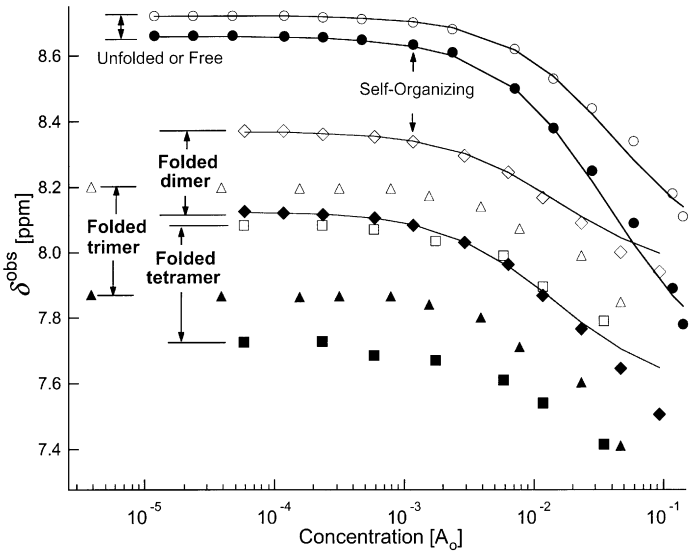

Figure 3. Plot of the observed chemical shifts Ha (open) and Hb (filled) of monomer **1** (circles), dimer **2** (diamonds), trimer **3b** (triangles), tetramer **4b** (squares) as a function of the initial molar concentration of each species. The chemical shift separation between Ha and Hb is very small for free monomer below self-assembly critical concentration ($C_C = 1$ mM) and is very large for the folded oligomers **2b**–**4b**; this effect is caused by the ring current of the π-stacked perylene neighbors. Theoretically, as concentrations approach infinity, the chemical shifts of Ha and Hb should approach constants corresponding to the limiting values of infinitely long nanowires made of perylene stacks.

Of particular significance is that all oligomers adopt a folded nanostructures within the concentration range studied by NMR and UV/Vis spectroscopy (1 μM to 0.1M). Another significant observation is that the folded nanostructures can further self-assemble into larger structures, and the critical concentration for folded oligomers to self-assemble is again $C_C = \sim 1$ mM, which is essentially same as the critical concentration of the monomer.

Photoluminescence Properties of Folded Polymers

The remarkable characteristic of chromophoric folded polymers is that the folded states emit photoluminescence of completely different colors from that of the unfolded states or free monomers. As discussed in the optical-absorption section, both folded and self-assembled π-stacks promote the PTD absorption shift from $0 \rightarrow 0$ transition (530 nm) to $0 \rightarrow 1$ transition (500 nm). This is attributed to shifts of the maximum overlap of Franck–Condon integral from $\langle \chi_{v'=0} | \chi_{v=0} \rangle$ in free monomers to $\langle \chi_{v'=0} | \chi_{v=1} \rangle$ in the folded nanostructures. As the folded chromophoric oligomers become larger, the photoluminescence favors emissions to higher vibronic ground states ($v' = 0 \rightarrow v$, $v = 0, 1, 2, 3$), thereby red-shifting the spectra. Representative examples of the photoluminescence of the folded PTD oligomers at 100 μM concentration are shown in Figure 4. This concentration is below the critical concentration for self-assembly (C_C), and therefore the photoluminescence shifts are largely due to folding of the PTD chromophores.

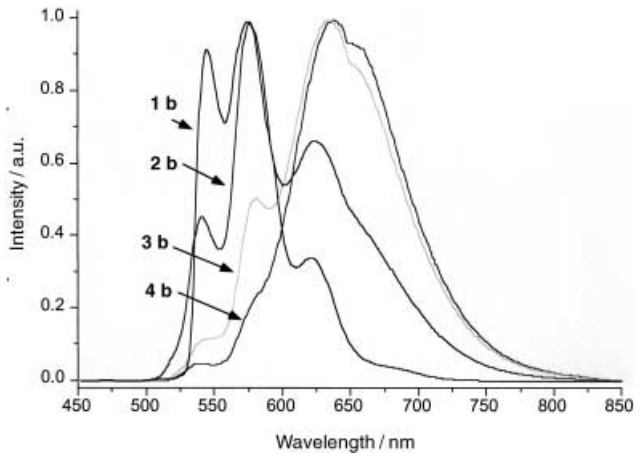

Figure 4. Photoluminescence of monomer **1b**, dimer **2b**, trimer **3b**, and tetramer **4b** at 100 μM concentration, which is below the critical concentration for self-organization; all spectra were obtained in chloroform with excitation at 429 nm.

In Figure 4, the monomer (**1b**) has dominant emission at 540 nm ($0 \rightarrow 0$) and 575 nm ($0 \rightarrow 2$), which make the monomer fluorescence green to yellow. For the dimer (**2b**), the green photoluminescence peak diminishes while the emission at 625 nm ($0 \rightarrow 3$) increases significantly; the combination of these three color photons yields an overall orange-red fluorescence. As the folded oligomers become larger, for instance trimer (**3b**) and tetramer (**4b**), the photoluminescence at green (540 nm) and yellow (575 nm) disappears quickly and the net emission color becomes more and more red. Notice that the red shift from trimer to tetramer is not significant but the reduction in yellow component (575 nm) is significant. The complete picture is that the monomer emits green light while the dimer emits orange and higher oligomers emit increasingly red light. A natural extension of this research is to add smart functions to the foldable polymers and utilize the color changes to construct chemical and biological sensors.[22]

Conclusion

Both folding and self-assembly are governed by the interactions between molecular units, either intramolecularly or intermolecularly. Each molecular unit generates a characteristic force field, and the radius of PTD force field is ~9–12 nm. When one molecular unit enters the force field of another molecular unit, the probability [Eq. (1)] of their

© 2003 Wiley-VCH Verlag GmbH & Co. KGaA, Weinheim

interacting will be significantly increased. The consequences of such interactions are manifested either as folding or self-assembling phenomena. This argues that the two molecular units have to be in close proximity for measurable interactions to occur. For PTD molecules, we measured a critical concentration of $C_C \sim 1$ mM for molecular association to occur. This hypothesis explains the folding phenomena in the alternating PTD and tetra(ethylene glycol) sequence as well as the critical concentration (C_C) for self-assembling of PTD derivatives.

$$P_{AB} \propto K' f_{AB} \approx \frac{K}{R_{AB}^{N}} \quad (1)$$

In other words, the probability (P_{AB}) of two molecular units, A and B, interacting with each other is proportional to their attractive force (f_{AB}), which is inversely proportional to R_{AB}^{N}, where R_{AB} the distance separating these two molecular units.

The forces that contribute to the force field include van der Waals force, Coulomb interaction, hydrogen bonding, and molecular-orbital overlap. They can be classified as either short-range interactions, like the van der Waals force and molecular-orbital overlap, or long-range interactions, such as the Coulomb interaction. Examples of known N are 2 for the Coulomb attraction and 6 for van der Waals' attraction.

The significance of understanding folding and self-assembly is that this knowledge provides remarkable power in designing useful molecular machinery, such as macromolecular biosensors and nano-actuators. These macromolecular biosensors and nano-actuators will play important roles in the future development of nanotechnology and biotechnology.

Acknowledgements

We acknowledge the support of the U.S. Department of Energy (D.O.E.) Los Alamos: sub-contract (28893-001-01-35), D.O.E. Office of Basic Energy Sciences: Division of Materials Science and Engineering. Pacific Northwest National Laboratory is a multiprogram national laboratory operated for the U.S.D.O.E. by the Battelle Memorial Institute under Contract DE-AC06-76RL0 1830.

[1] J. G. Saven, *Chem. Rev.* **2001**, *101*, 3113, and references therein.
[2] G. M. Blackburn, G. Walcher, *Pol. J. Chem*. **2001**, *75*, 1183.
[3] A. K. Ogawa, Y. Q. Wu, D. L. McMinn, J. Q. Liu, P. G. Schultz, F. E. Romesberg, *J. Am. Chem. Soc.* **2000**, *122*, 3274.
[4] V. Berl, I. Huc, R. G. Khoury, M. J. Krische, J.-M. Lehn, *Nature* **2000**, *407*, 720.
[5] J. Recker, D. J. Tomcik, J. R. Parquette, *J. Am. Chem. Soc.* **2000**, *122*, 10298.
[6] J. Q. Nguyen, B. L. Iverson, *J. Am. Chem. Soc*. **1999**, *121*, 2639.
[7] R. B. Prince, S. A. Barnes, J. S. Moore, *J. Am. Chem. Soc.* **2000**, *122*, 2758.
[8] A. J. Zych, B. I. Iverson, *J. Am. Chem. Soc.* **2000**, *122*, 8898.
[9] D. G. Lidzey, D. D. C. Bradley, S. F. Alvarado, P. F. Seidler, *Nature* **1997**, *386*, 135.
[10] Y. Cao, I. D. Parker, G. Yu, C. Zhang, A. J. Heeger, *Nature* **1999**, *397*, 414.
[11] F. Hide, M. A. Diaz Garcia, B. J. Schwartz, M. R. Andersson, Q. B. Pei, A. J. Heeger, *Science* **1996**, *273*, 1833.
[12] J. Kim, T. M. Swager, *Nature* **2001**, *411*, 1030.
[13] D. T. McQuade, A. H. Hegedus, T. M. Swager, *J. Am. Chem. Soc.* **2000**, *122*, 12389.
[14] T. Q. Nguyen, J. J. Wu, V. Doan, B. J. Schwartz, S. H. Tolbert, *Science* **2000**, *288*, 652.
[15] H. Sirringhaus, P. J. Brown, R. H. Friend, M. M. Nielsen, K. Bechgaard, B. M. W. Langeveld-Voss, A. J. H. Spiering, R. A. J. Janssen, E. W. Meijer, P. Herwig, D. M. de Leeuw, *Nature* **1999**, *401*, 685.
[16] A. Devasagayaraj, J. M. Tour, *Macromolecules* **1999**, *32*, 6425.
[17] K. Oh, K. S. Jeong, J. S. Moore, *Nature* **2001**, *414*, 889.
[18] G. W. Orr, L. J. Barbour, J. L. Atwood, *Science* **1999**, *285*, 1049.
[19] S. Lahiri, J. L. Thompson, J. S. Moore, *J. Am. Chem. Soc*. **2000**, *122*, 11315.
[20] R. B. Prince, S. A. Barnes, J. S. Moore, *J. Am. Chem. Soc*. **2000**, *122*, 2758.
[21] W. Wang, W. Wan, H.-H. Zhou, S. Q. Niu, A. D. Q. Li, *J. Am. Chem. Soc*. **2003**, *125*, 5248.
[22] W. Wang, L.-S. Li, G. Helms, H.-H. Zhou, A. D. Q. Li, *J. Am. Chem. Soc*. **2003**, *125*, 1120.
[23] B. Frisch, C. Boeckler, F. Schuber, *Bioconjugate Chem*. **1996**, *7*, 180.
[24] H. Langhals, H. Jaschke, U. Ring, P. von Unold, *Angew. Chem.* **1999**, *111*, 143; *Angew. Chem. Int. Ed*. **1999**, *38*, 201.
[25] M. S. Cubberley, B. L. Iverson, *J. Am. Chem. Soc*. **2001**, *123*, 7560.
[26] M. Kataoka, Y. Hayakawa, *J. Org. Chem*. **1999**, *64*, 6087.
[27] C. C. Ling, A. W. Coleman, M. Miocque, *Carbohydr. Res.* **1992**, *223*, 287.
[28] R. W. Sobol, E. E. Henderson, N. Kon, J. Shao, P. Hitzges, E. Mordechai, N. L. Reichenbach, R. Charubala, H. Schirmeister, W. Pfleiderer, R. J. Suhadolnik, *J. Biol. Chem.* **1995**, *270*, 596.
[29] Y. Hayakawa, R. Kawai, A. Hirata, J. Sugimoto, M. Kataoka, A. Sakakura, M. Hirose, R. Noyori, *J. Am. Chem. Soc*. **2001**, *123*, 8165.
[30] H. Langhals, R. Ismael, *Eur. J. Org. Chem*. **1998**, 1915.
[31] W. E. Ford, *J. Photochem*. **1987**, *37*, 189.
[32] W. Wang, J. J. Han, L.-Q. Wang, L.-S. Li, W. J. Shaw, A. D. Q. Li, *Nano Lett.* **2003**, *3*, 455–458.

 © 2003 Wiley-VCH Verlag GmbH & Co. KGaA, Weinheim